Getting to know the nitrogen next door: HNMBC measurements of amino sugars

John F.K. Limtiaco [a], Derek J. Langeslay [a], Szabolcs Beni [a,b], Cynthia K. Larive [a,*]

[a] Department of Chemistry, University of California – Riverside, Riverside, CA 92521, United States
[b] Semmelweis University, Department of Pharmaceutical Chemistry, Hőgyes Endre u. 9, H-1092 Budapest, Hungary

ABSTRACT

Long-range ^{1}H–^{15}N correlations detected by the heteronuclear multiple-bond correlation (HMBC) experiment are explored for the characterization of amino sugars. The gradient-enhanced HMBC, IMPACT-HMBC, and a modified pulse sequence with the ^{1}J-filters removed, IMPACT-HNMBC, are compared for sensitivity and resolution. ^{15}N chemical shifts and long-range proton correlations are reported using the IMPACT-HNMBC experiment for N-acetyl-glucosamine, N-acetyl-galactosamine, and for a series of glucosamine analogs with an N-sulfo substitution, unmodified amino group, and 6-O-sulfonation. As is common with sugars, for all the compounds examined both anomeric forms are present in solution. For each compound studied, the ^{15}N chemical shifts of the α anomer are downfield of the β form. For the N-acetylated sugars, the β anomer has a unique long-range ^{15}N correlation to the anomeric proton not observed for the α anomer. Though N-sulfonation results in a significant change in the ^{15}N chemical shift of the glucosamine analogs, 6-O sulfo substitution has no significant effect on the local environment of the amino nitrogen. For N-acetylated sugars in D$_2$O solution, peaks in the ^{15}N projection of the HMBC spectrum appear as triplets as a result of J-modulation due to ^{2}H–^{15}N coupling.

© 2011 Elsevier Inc. All rights reserved.

1. Introduction

Amino sugars are important components of many natural products including antibiotics, carbohydrate-based vaccines, and glycosaminoglycans (GAGs). GAGs are a class of linear anionic polysaccharides that include chondroitin sulfate, dermatan sulfate, heparin, heparan sulfate, keratan sulfate, and hyaluronic acid. Heparin and heparan sulfate (HS) are structurally the most complex members of the GAG family. Although heparin and HS are biosynthesized through a common backbone of repeating glucuronic acid (GlcA) (1 → 4) N-acetyl-D-glucosamine (GlcNAc) disaccharide building blocks, the end products are both polydisperse and microheterogeneous [1]. This structural heterogeneity arises through the action of specific sulfotransferase enzymes which introduce variable N-sulfo, 2-O and 6-O-sulfo substitutions and an epimerase which partially inverts the configuration of the GlcA residue to form iduronic acid (IdoA). Chondroitin sulfate has a more regular structure than heparin or HS, with the uronic acid residue exclusively as GlcA and all of the galactosamine residues present in the N-acetylated form (GalNAc). Sulfotransferase enzymes introduce variability in chondroitin sulfate in the form of GlcA 2-O and GalNAc 4-O and 6-O-sulfonation.

Despite the biological importance of heparin, HS, chondroitin sulfate and the other GAGs [2,3] until recently relatively little

information had been reported about the ^{15}N chemical shifts of the amino sugars in these biopolymers. The low natural abundance of ^{15}N, its negative NOE and long T_1 relaxation times make direct detection of ^{15}N spectra challenging. These limitations are easily overcome by inverse experiments, for example heteronuclear single-quantum coherence (HSQC) spectroscopy, which detect ^{15}N through the resonances of directly-bonded protons [4–6]. There are several examples of the use of HSQC to characterize GAG-derived materials. The HSQC experiment has been used to characterize ^{15}N-labeled heparosan, a biopolymer with repeating (GlcA–GlcNAc) disaccharide residues biosynthesized through bacterial expression systems [7–9]. Blundell et al. reported the complete ^{1}H, ^{13}C and ^{15}N resonance assignments at 900 MHz for a family of hyaluronic acid oligosaccharides at natural abundance. These authors used [^{1}H–^{15}N]-HSQC spectra to distinguish the position of the hyaluronic acid GlcNAc residues within a hexasaccharide chain, with separate signatures obtained from terminal and internal GlcNAc ^{15}N nuclei [9]. In a recent report, Pomin et al. used HSQC for detection of ^{15}N-labeled GalNAc from chondroitin sulfate and dermatan sulfate, and GlcNAc from HS isolated from cultured mouse lung endothelial and CHO cells to which ^{15}N-labeled glutamine was added as a precursor [10]. Pomin et al. noted that HSQC experiments with HS were less useful for structural characterization, as only the GlcNAc residues could be detected by this approach [10]. Although these authors were unable to detect the ^{15}N resonances of either the GlcNS or GlcN residues of HS because of the fast exchange of the nitrogen-bonded protons with water,

* Corresponding author. Fax: +1 951 827 4713.
E-mail address: clarive@ucr.edu (C.K. Larive).

Zhang et al. reported detection of a very weak resonance assigned to GlcNS in the HSQC spectrum of uniformly $^{13}C/^{15}N$ labeled N-sulfo heparosan in D_2O [11].

An alternative strategy explored in this study is the use of *h*eteronuclear *m*ultiple-*b*ond *c*orrelation (HMBC) experiments to detect ^{15}N chemical shifts through long-range couplings. Such [^1H–^{13}C]-HMBC experiments are widely employed in the structural characterization of organic compounds [6,12–14]. Although applications of [^1H–^{15}N]-HMBC are less prominent in the literature,

characterization of nitrogen containing natural products using this approach is well-accepted and has been the subject of a thorough review by Martin and Hadden [15]. The goal of this work was to demonstrate the detection of ^{15}N chemical shifts for a family of amino sugars with a variety of structures through long-range couplings to the carbon-bonded protons of the glucosamine ring. In the process of performing these measurements three pulse sequences were compared and an optimized set of experimental parameters was determined.
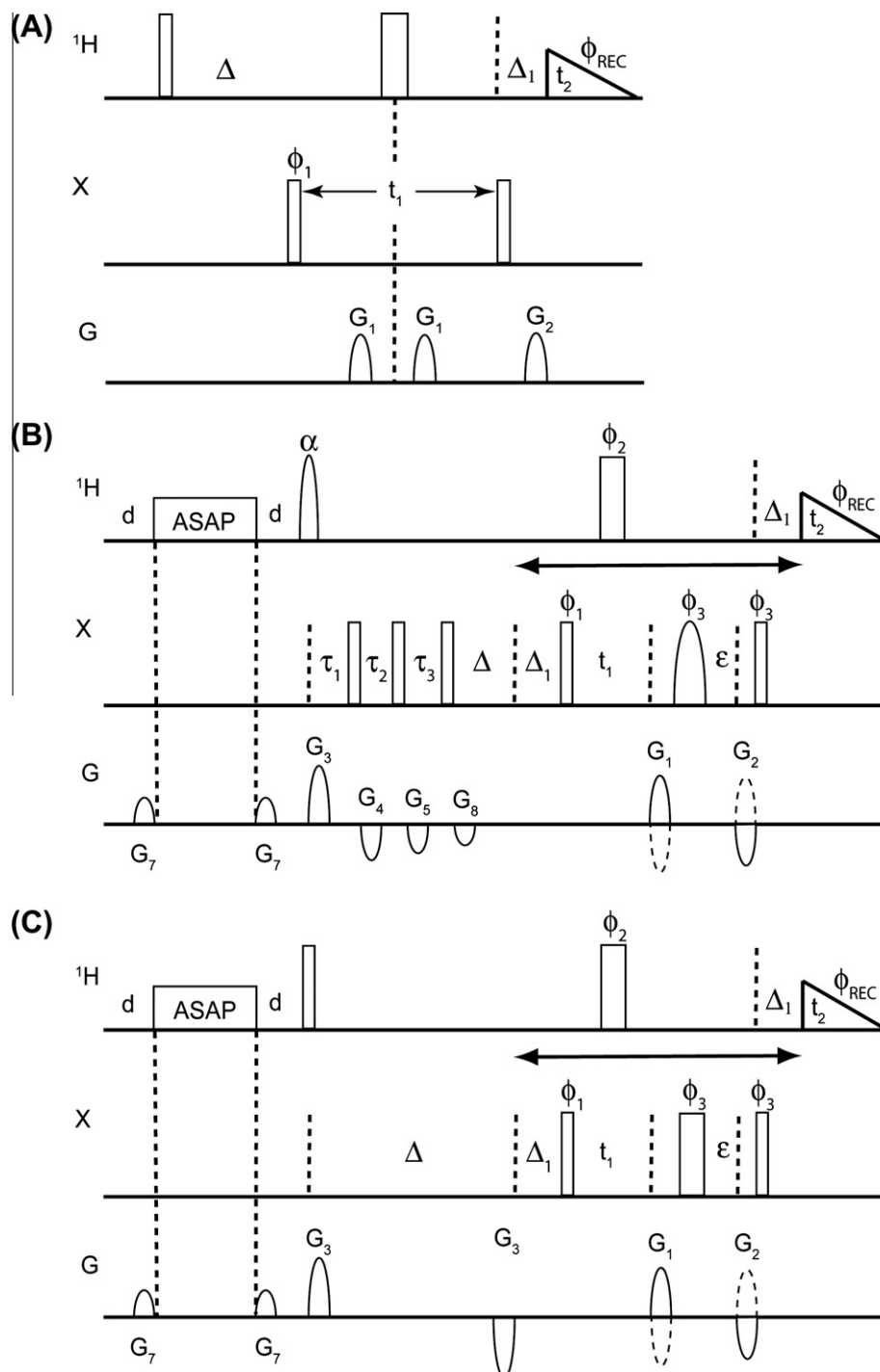

Fig. 1. The NMR pulse sequences for the (A) ge-HMBC, (B) IMPACT-HMBC, and (C) IMPACT-HNMBC experiments. Narrow open bars indicate 90° pulses and wider bars 180° pulses. In the IMPACT-HNMBC pulse sequence, the first pulse on the ^1H channel, originally a sine shaped pulse, is replaced by a broadband 90° pulse while the 180° pulse on the ^{15}N channel was either a broadband or band-selective Q3 Gaussian pulse. Additionally, the three step low-pass ^1J filter was removed in order to reduce T_2 losses and improve the S/N.

2. Methods

The sugars examined in this study all contained ^{15}N at natural abundance levels. D-glucosamine (GlcN) hydrochloride and N-acetyl-D-glucosamine-6-O-sulfate (GlcNAc6S) were purchased from Sigma–Aldrich (St. Louis, MO). N-sulfo-D-glucosamine (GlcNS), N-sulfo-D-glucosamine-6-O-sulfate (GlcNS6S), and D-glucosamine-6-O-sulfate (GlcN6S) were purchased from V-Labs (Covington, LA). N-acetyl-D-glucosamine (GlcNAc) was purchased from Alfa Aesar (Ward Hill, MA) while N-acetyl-D-galactosamine (GalNAc) was purchased from Acros Organics (Geel, Belgium). The lyophilized powders were reconstituted in D_2O and the solution pD adjusted to 7.40 with 0.1 M DCl and NaOD. Sodium 3-(trimethylsilyl)propionate-2,2,3,3-d4 (TMSP, Cambridge Isotope Laboratories) was
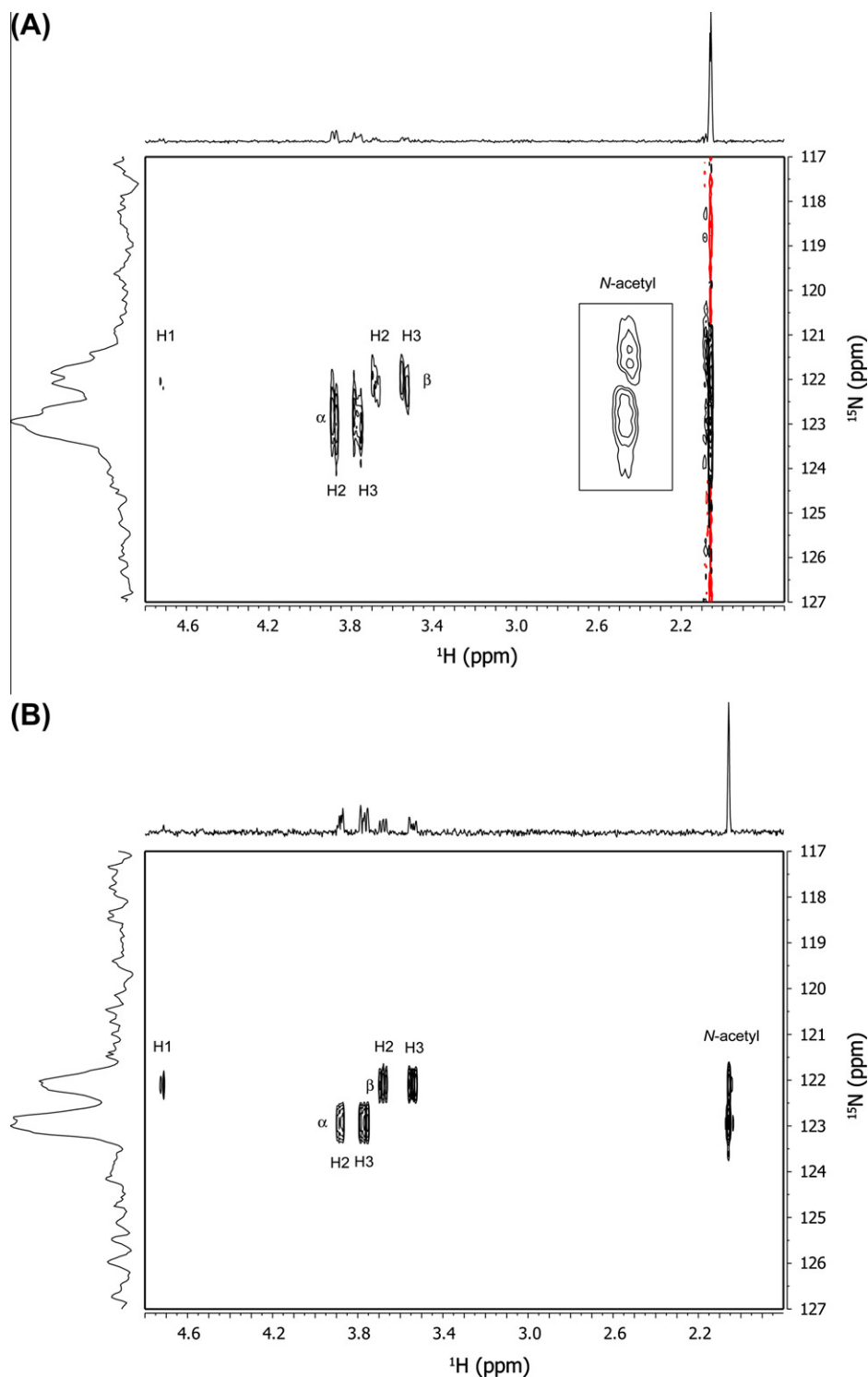

Fig. 2. Two-dimensional HMBC NMR spectra of GlcNAc recorded on a 600 MHz NMR spectrometer using the (A) ge-HMBC, (B) IMPACT-HMBC, and (C) IMPACT-HNMBC pulse sequences. Spectra were recorded using 128 increments and 32 transients with a spectral window of 3004 Hz in F_2 and 1215 Hz in F_1. The measurement time for each of the experiments was approximately 3 h.
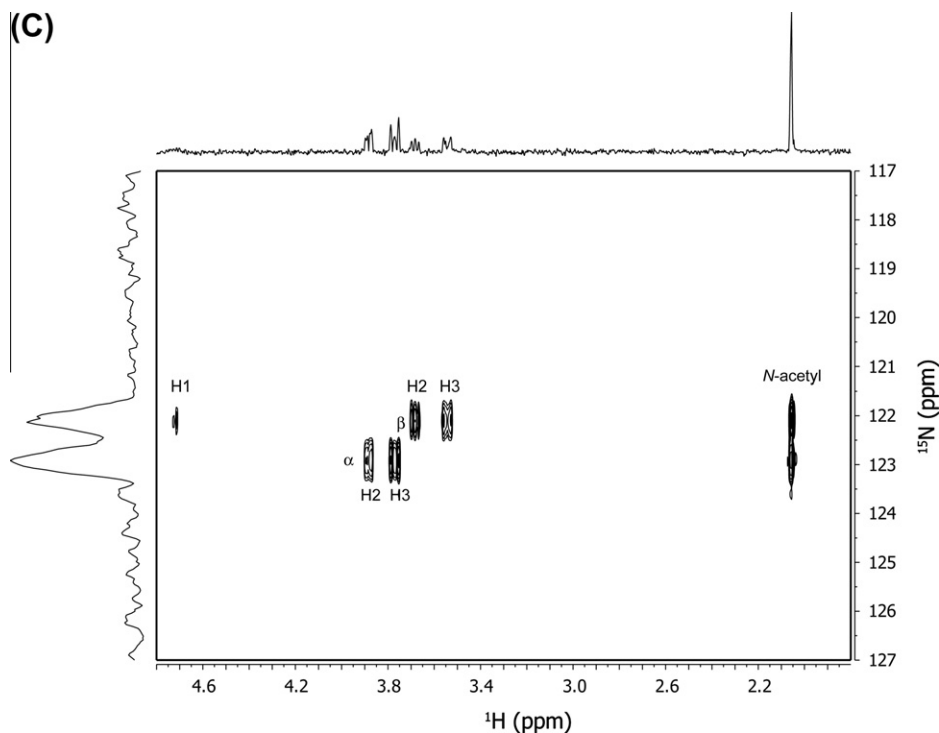
Fig. 2 (*continued*)

added as an internal chemical shift reference (0 ppm) and the samples diluted as needed to give a final concentration between 100 and 500 mM.

NMR spectra were recorded at 25 °C using a Bruker Avance spectrometer operating at 599.84 MHz for ^{1}H and 60.79 MHz for ^{15}N. All NMR experiments were performed using a broad-band inverse probe with x, y, and z gradients. ^{1}H NMR spectra were acquired with 64 transients into 32,768 data points using a 6.6 kHz spectral window and a 2 s relaxation delay. Proton survey NMR spectra were acquired using presaturation to suppress the residual HOD resonance and were processed using Topspin version 1.3. Prior to Fourier transformation, the free induction decays (FIDs) were zero-filled to 65,536 points and apodized by multiplication with an exponential function equivalent to 0.5 Hz line broadening.

[^{1}H–^{15}N]-HMBC spectra were acquired with an acquisition time of 0.3408 s and a relaxation delay of 2.0 s. Initial parameter sets were optimized with GlcNAc, since the ^{15}N chemical shift of this monosaccharide is easily detected by HSQC. A sample of 500 mM GlcNAc in D$_2$O was used to compare the different pulse sequences. For the glucosamine mixture solution each of the components, GlcN, GlcNAc, and GlcNS was present at a concentration of 100 mM. To facilitate detection of sugar resonances close to the solvent peak, D$_2$O was selected as the solvent for most measurements. For the pulse sequence comparison, 32 scans were acquired into 2048 data points in F_2 with 128 t_1 increments using spectral widths of 3004 Hz and 1215 Hz in the ^{1}H and ^{15}N dimensions, respectively.

The IMPACT-HNMBC (*i*mproved and *a*ccelerated *c*onstant-*t*ime *p*roton *n*itrogen *m*ultiple-*b*ond *c*orrelation) spectrum of the glucosamine mixture was acquired with 512 t_1 increments and a spectral width of 3004 Hz and 9115 Hz in the ^{1}H and ^{15}N dimensions, respectively. A total of 32 scans were acquired for each increment. Subsequent spectra for the GlcN analogs at a concentration of 200 mM were acquired with 220 t_1 increments and a spectral width of 1215 Hz in the ^{15}N dimension. For the GalNAc sample at

500 mM, 32 scans were acquired into 2048 data points in F_2 and 256 t_1 increments using a spectral width of 3004 Hz and 1215 Hz in the ^{1}H and ^{15}N dimensions, respectively. An IMPACT-HNMBC spectrum of GalNAc (643 mM) was also measured in 90% H$_2$O/ 10% D$_2$O (Supplemental Fig. 1) using 74 scans into 2048 data points in F_2 and 256 t_1 increments. The HSQC spectrum of 250 mM GalNAc in 90% H$_2$O/10% D$_2$O was acquired with 80 scans into 2048 data points in F_2 and 300 t_1 increments with a spectral width of 6009 Hz and 1215 Hz in the ^{1}H and ^{15}N dimensions, respectively. For purposes of ^{1}H resonance assignment, DQF-COSY spectra were acquired for all samples with 16 transients into 2048 data points in the F_2 dimension and 256 t_1 increments. COSY spectra were measured with a spectral width of 3 kHz and an acquisition time of 0.3408 s per t_1 increment.

Data processing of 2D spectra was performed using the MestReNova NMR suite version 6.2.0 (Santiago de Compostela, Spain). Spectra were apodized in both dimensions with a sine-bell function shifted by 90° and zero-filled in the F_1 dimension to 1024 data points. Indirect referencing in the ^{15}N dimension was accomplished using the TMSP resonance in the ^{1}H NMR spectra [16]. The signal-to-noise ratios for comparison of the IMPACT-HMBC and IMPACT-HNMBC experiments were determined using the Topspin signal-to-noise processing command (SINO). The signal-to-noise ratios were calculated by summing the projections along F_2 for both the α (122.83 ppm) and β (122.11 ppm) anomers of GlcNAc [17,18].

3. HMBC pulse sequences

The HMBC experiment is a powerful tool for structure elucidation of synthetic compounds and natural products. It allows connections to be made from protons via long-range couplings to carbon nuclei, even those without directly-bonded protons such as carbonyl carbons and the quaternary carbons of phenyl rings. A common strategy in structure elucidation is to identify molecular building blocks using homonuclear ^{1}H–^{1}H couplings to assign the
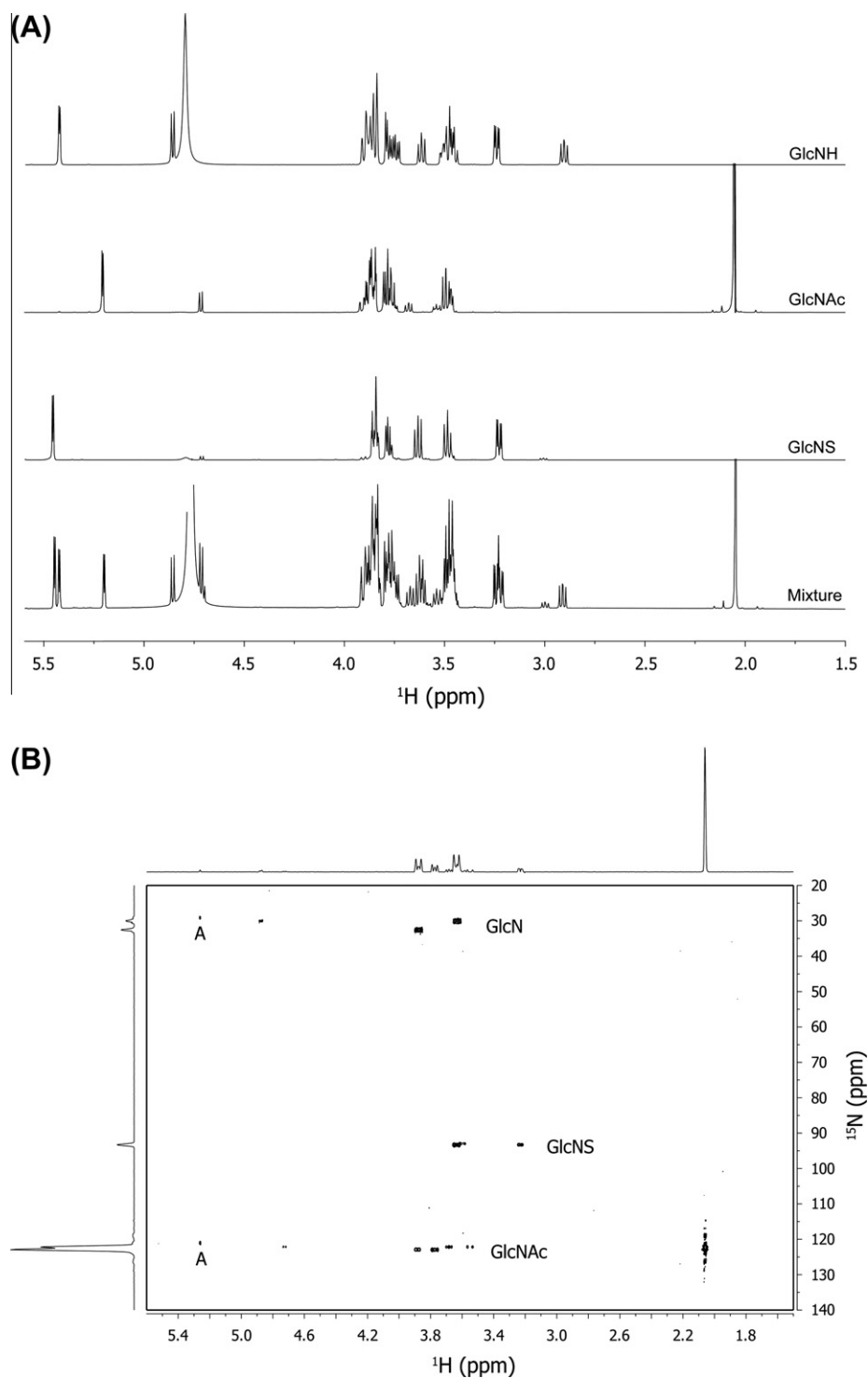
Fig. 3. (A) ^{1}H NMR spectra, (B) IMPACT-HNMBC spectrum of a mixture containing GlcN, GlcNS, and GlcNAc each at a concentration of 100 mM in D_2O. The IMPACT-HNMBC spectrum was acquired with a spectral width of 3004 Hz in the ^{1}H dimension and 9115 Hz in the ^{15}N dimension in 12 h. The weak cross peaks labeled A in the IMPACT-HNMBC spectrum correspond to spectral artifacts that are not present in the spectrum of the mixture (A) or in the IMPACT-HNMBC spectra acquired for solutions of the individual amino sugars.

resonances within spin systems, and then to stitch the spin systems together using a combination of [^{1}H–^{13}C]-HSQC and HMBC correlations. In this process, one-bond couplings are identified in the HSQC spectrum and correlated with the longer-range HMBC connectivities. Because the HMBC spectra reveal connections through two, three, or occasionally four bonds, the spectra can be crowded and one-bond filters are often incorporated to suppress the cross peaks from directly-bonded protons. A commonly implemented version of this experiment is the gradient-enhanced (ge)-HMBC pulse sequence shown in Fig. 1A [19–21].

For complex structures or crowded spectra, the poor digital resolution in the F_1 dimension of the 2D HMBC spectrum can make it difficult to resolve ^{13}C resonances that are close in chemical shift. This problem can be subverted using a band selective version of the experiment in which only the crowded ^{13}C spectral region of interest is excited and the spectrum is acquired with greater F_1
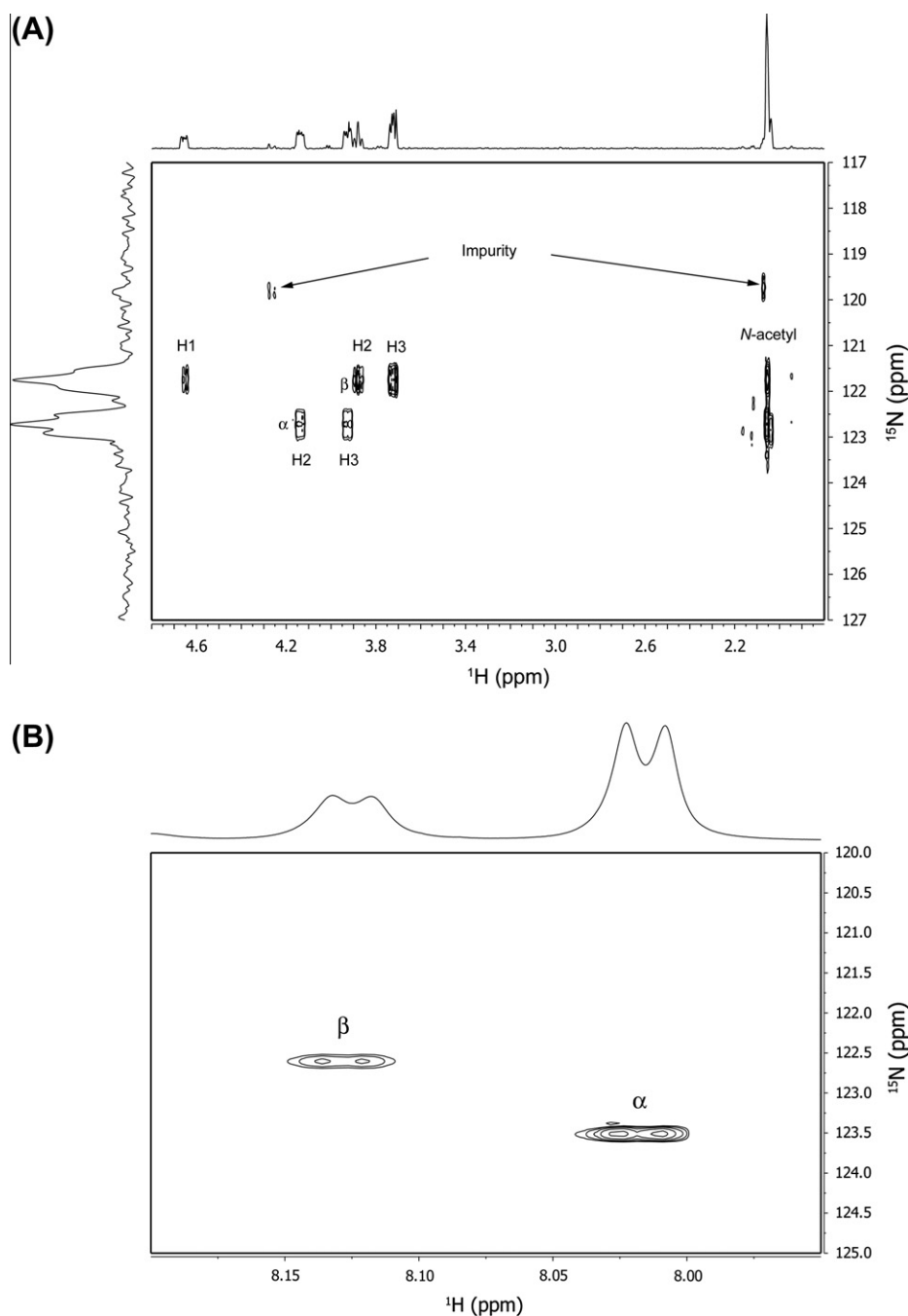
Fig. 4. Two-dimensional NMR spectra of GalNAc: (A) IMPACT-HNMBC at 500 mM GalNAc in D_2O, (B) portion of the HSQC, and (C) DQF-COSY at 250 mM in 90% H_2O/10% D_2O, confirming the assignment of the α and β anomeric forms.

digital resolution. However, if this approach is used, skewing of the cross peaks is observed as a result of proton J-coupling modulation. Claridge and Perez-Victoria introduced a band-selective constant-time (CT) pulse sequence that eliminates this modulation due to homonuclear couplings, greatly improving the resolution of cross peaks in the resulting CT-HMBC spectrum [22]. Building on this idea, Furrer recently reported the IMPACT-HMBC (*imp*roved and *a*ccelerated *c*onstant-*t*ime *h*eteronuclear *m*ultiple-*b*ond *c*orrelation) experiment illustrated in Fig. 1B [23]. The IMPACT-HMBC pulse sequence uses a constant-time evolution period to minimize cross peak skew introduced by evolution of ^{1}H–^{1}H couplings during the 1/(2 J) delay and incorporates an ASAP period that reduces F_1 noise while enhancing sensitivity by minimizing the recycle delay used in this experiment.

The goal of this study is to measure ^{15}N chemical shifts of amino sugars through long-range ^{1}H–^{15}N couplings. While the pulse sequences shown in Fig. 1A and B can be used to measure [^{1}H–^{15}N]-HMBC spectra, they are not ideal. Because the long-range ^{1}H–^{15}N couplings we hope to detect are very small (2–3 Hz), skew from ^{1}H–^{1}H J-modulation should be even more pronounced than in ^{1}H–^{13}C experiments, so a constant-time experiment should be beneficial. In [^{1}H–^{15}N]-HMBC spectra we do not expect interferences from one-bond couplings and removal of the ^{1}J-filters should improve sensitivity [24]. Fig. 1C illustrates a modified pulse sequence we refer to as IMPACT-HNMBC, following the convention of Farley et al. [24] and Williamson et al. [25]. In this pulse sequence, the filters designed to suppress one-bond couplings have been eliminated and the gradient pulses contained within these filters
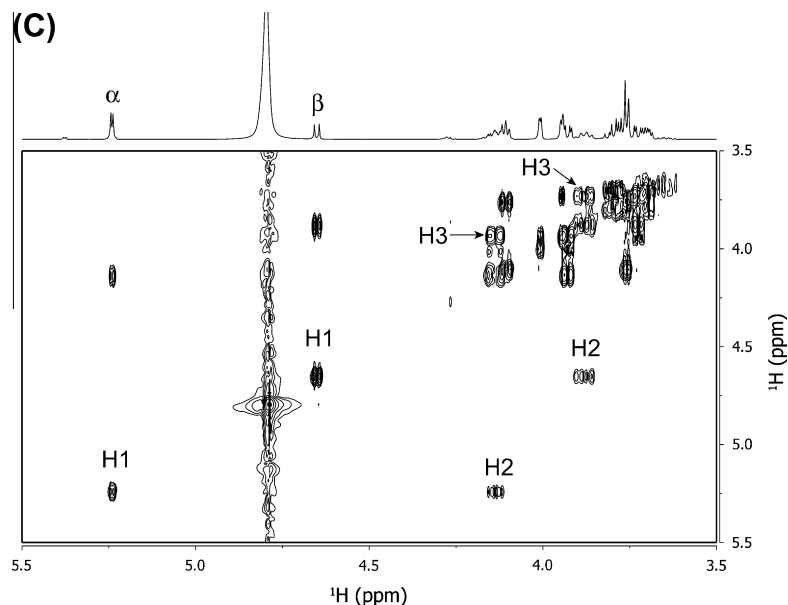
Fig. 4 (*continued*)

collapsed into a single gradient pulse. Although Fig. 1C shows the pulse sequence with a non-selective 180° nitrogen inversion pulse, a band-selective pulse can be substituted if greater selectivity in the ^{15}N dimension is desired.

4. Results

Fig. 2 shows the results obtained for the pulse sequences illustrated in Fig. 1 using a D$_2$O solution containing 500 mM GlcNAc at ^{15}N natural abundance. Each spectrum was acquired using identical parameters with a total acquisition time of 3 h for each experiment. These spectra contain several long-range ^{1}H–^{15}N correlations. Fig. 2A shows the spectrum produced by the ge-HMBC pulse sequence. Strong cross peaks are observed for the *N*-acetyl protons with weaker cross peaks to the H2 and H3 protons of the sugar ring. The two ^{15}N chemical shifts result from the presence of α and β GlcNAc anomers. As shown in the insert in Fig. 2A because of the singlet nature of the *N*-acetyl resonance, these cross peaks are not susceptible to skewing. However, the cross peaks to the H2 and H3 protons of the glucosamine ring show a strong variation with proton chemical shift due to ^{1}H–^{1}H coupling modulation.

Fig. 2B shows the results obtained with the IMPACT-HMBC pulse sequence. The ASAP feature of this pulse sequence greatly reduces the F_1 noise ridges from the *N*-acetyl singlet resonance. Compared with the ge-HMBC results in Fig. 2A, this constant-time pulse sequence provides improved sensitivity and resolution in the ^{1}H dimension by eliminating cross peak skew due to ^{1}H–^{1}H coupling [26]. As expected, the ^{15}N projection in Fig. 2B now contains only two nitrogen peaks, due to the α and β anomers. For the β-anomer, the cross peak between ^{15}N and H1, clearly detected in Fig. 2B, appears to be only noise in the ge-HMBC spectrum in Fig. 2A. Removal of the one-bond *J*-filters in the IMPACT-HNMBC pulse sequence further enhances the signal-to-noise ratio (S/N) of the spectrum shown in Fig. 2C by reducing transverse relaxation losses. Although it can be difficult to assess sensitivity gains from the contour plots alone, the projections in the ^{1}H dimension reflect the S/N improvements provided by the IMPACT-HNMBC pulse sequence when compared with the ge-HMBC and IMPACT-HMBC experiments. Signal-to-noise improvements ranging from 7% to

36% were observed for the cross peaks in the IMPACT-HNMBC spectrum when compared to the IMPACT-HMBC spectrum acquired in the same amount of time. It is expected that improvements in signal intensity from the IMPACT-HNMBC experiment would be more pronounced when investigating larger compounds or more viscous solutions where greater transverse relaxation losses are expected [27].
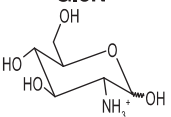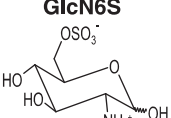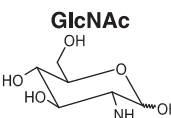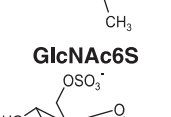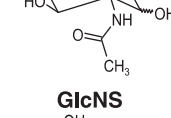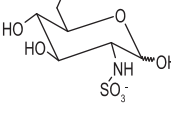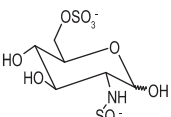
Although the results shown in Fig. 2C are promising, the ^{15}N chemical shift of GlcNAc could have been more easily measured using the HSQC experiment. The potential power of this approach is in the detection of ^{15}N chemical shifts through long-range ^{1}H–^{15}N couplings in situations where rapid chemical exchange prevents detection of the directly-bonded protons using HSQC. Therefore, to test the utility of the IMPACT-HNMBC experiment, we prepared a solution containing three glucosamine analogs, Glc-NAc, GlcNS and GlcN, each at a concentration of 100 mM. Fig. 3A shows the ^{1}H NMR spectra of these compounds individually and as a mixture. The spectrum of the mixture aptly illustrates the problem of proton resonance overlap due to the limited dispersion common in carbohydrate NMR.

Shown in Fig. 3B is the IMPACT-HNMBC spectrum measured for the mixture of glucosamine analogs at a concentration of 100 mM for each component. This spectrum was acquired using an evolution delay of 167 ms, corresponding to an average coupling constant of 3.0 Hz. The sensitivity of the ^{15}N chemical shift to nitrogen substitution is quite dramatic. The ^{15}N chemical shifts observed for this solution ranged from 122.83 ppm (α) and 122.11 (β) for GlcNAc, to 32.49 (α) and 29.93 (β) for GlcN. To our knowledge, this is the first report of the ^{15}N chemical shift of GlcN measured in solution, although Tzou reported ^{15}N chemical shifts for the amino form of GlcN of 16.9 (α) and 15.0 (β) using solid state NMR [28]. For GlcNS the α anomer was observed with a ^{15}N chemical shift of 93.21 ppm while the less intense β anomer was observed at 92.90 ppm. Compared with Fig. 3A, the ^{1}H projection is greatly simplified since only those protons within 2 or 3 bonds of the ^{15}N are detected. It is also interesting that the different glucosamine analogs show different coupling patterns to nearby glucosamine ring protons.

Although it appears from the ^{15}N projection in Fig. 3B that the sensitivity of the experiment is greater for GlcNAc than for GlcNS or GlcN, this is an artifact of the intense GlcNAc *N*-acetyl

Table 1
Amino sugar ^{15}N chemical shifts and long-range ^{1}H correlations observed in the IMPACT-HNMBC spectra measured in D$_2$O solution.

Amino sugar	Anomer	^{15}N	H1	H2	H3	N-acetyl
GlcN	α	32.49			3.874	
	β	29.93	4.873[a]		3.631	
GlcN6S	α	32.35			3.879	
	β	29.71			3.626	
GlcNAc	α	122.83		3.88	3.768	2.056
	β	122.11	4.716	3.68	3.546	2.054
GlcNAc6S	α	122.70		3.909	3.779	2.056
	β	121.97		3.706	3.56	2.056
GlcNS	α	93.21		3.229	3.634	
	β	92.90			3.596	
GlcNS6S	α	93.20		3.254	3.645	
	β	92.74			3.608	
GalNAc	α	122.78		4.137	3.926	2.057
	β	121.81	4.652	3.879	3.723	2.055

Chemical shift (ppm)

[a] Indicates a very weak signal, detected just above the noise floor.

resonance. If the projection is derived only from the glucosamine ring cross peaks, the intensities of the peaks in the ^{15}N projection are comparable. Two weak artifacts were also observed in the IM-PACT-HNMBC spectrum (Fig. 3B) as indicated. The ^{1}H NMR survey spectrum (Fig. 3A) of this sample showed no peak at the chemical shift of these cross peaks and we confirmed these cross peaks as artifacts using previously acquired IMPACT-HNMBC spectra of the individual components. We have previously reported that the population of the α and β anomers in heparin disaccharides depends on the nature of the substituent on the glucosamine nitrogen [29] and the results in Fig. 3B reinforce that conclusion. The ratio (β/α) measured using the anomeric proton resonances (Fig. 3A) for GlcN, GlcNS, and GlcNAc were 0.58, 0.05, and 0.68, respectively, a trend similar to that observed by Eldridge et al. in

the ^{1}H NMR spectra of heparin disaccharides [29]. In GlcNS the bulky N-sulfo substitution likely reduces the stability of the β anomer due to steric effects.

Fig. 4A shows the high-resolution IMPACT-HNMBC spectrum acquired for a solution of 500 mM GalNAc in D$_2$O with 256 t_1 increments using a spectral width of 1215 Hz in F_1. In addition to the detection of both the α and β anomers of GalNAc, we also detected a minor contaminant at a ^{15}N chemical shift of 119.73 ppm as shown in Fig. 4A. For comparison, the HSQC spectrum of GalNAc measured in 90% H$_2$O/10% D$_2$O is shown in Fig. 4B. As in the case of the glucosamine analogs, two ^{15}N chemical shifts are detected corresponding to the α and β anomeric forms of GalNAc. Comparison of the ^{15}N chemical shifts of GalNAc in 100% D$_2$O and 90% H$_2$O/10% D$_2$O reveals an upfield shift of 0.74 and 0.80 ppm for the α and β anomers, respectively as a result of deuterium substitution. This solvent-dependent difference in nitrogen chemical shifts has been reported previously following exchange of nitrogen-bound protons with ^{2}H in protein amide groups [30,31]. Based on the pattern of long-range couplings observed in Fig. 4A and its greater abundance, we initially assigned the more intense downfield ^{15}N resonance in Fig. 4B to the α anomer. The ^{1}H–^{1}H coupling constants measured for the GalNAc anomeric proton (H1) of 3.65 Hz (α) and 8.45 Hz (β) are also consistent with this assignment. After realizing that our assignment of the ^{15}N chemical shifts of the GalNAc anomers was opposite to that reported by Pomin et al., we measured a COSY spectrum of this solution (Fig. 4C) which confirmed our assignments. Our assignment of the downfield ^{15}N resonance to the α anomer is also consistent with the results reported for GalN by solid state NMR [28].

It is interesting that in the ^{15}N projection in Fig. 4A, each ^{15}N resonance appears as a triplet. Measurement of the IMPACT-HNMBC spectrum in 90% H$_2$O/10% D$_2$O (Supplemental Fig. 1) removes the coupling in F_1 and the ^{15}N projection of GalNAc shows only sharp singlet peaks. This is expected as constant-time experiments are specifically designed to refocus couplings involving protons. We also did not observe splitting of the ^{15}N projection in similar spectra acquired for the GlcN or GlcNS samples, where fast deuterium exchange is expected. Although this ^{15}N multiplicity is not well-resolved in Fig. 2C, acquisition of spectra with higher digital resolution in F_1 for D$_2$O solutions of GlcNAc and GlcNAc6S (Supplemental Fig. 2A and B, respectively) also produced triplets in the indirect dimension. We attribute this multiplicity to ^{2}H–^{15}N coupling and measured coupling constants of 12.6 Hz and 12.7 Hz for GalNAc and GlcNAc, respectively. Using an average ^{15}N–^{1}H coupling constant of 90 Hz [32], splitting patterns observed using IMPACT-HNMBC relate well to the ^1J coupling constants estimated for ^{15}N and ^{2}H of 13.8 Hz using $\gamma_H/\gamma_D \approx 6.5$. Although a 1:1:1 triplet pattern would normally be expected for coupling to a spin 1 nucleus like deuterium, in these spectra the center resonance of the triplet is of greater intensity than the two outer bands. These intensity variations are most likely due to differences in the quadrupolar relaxation of the different spin states of ^{2}H, which are compounded by the long ^{1}H–^{15}N coupling delay used in the HMBC experiment.

IMPACT-HNMBC spectra were also recorded for a series of glucosamine analogs selected to examine the effect of 6-O sulfonation, a common motif in heparin and HS, on ^{15}N chemical shift. Table 1 summarizes the ^{15}N chemical shifts obtained for all the compounds studied along with the chemical shifts of the protons detected by long-range ^{1}H–^{15}N correlations. Although the ^{15}N chemical shift of GalNAc and GlcNAc are quite similar, they can be easily distinguished by their ^{1}H chemical shifts. It is interesting that the β anomers of GlcNAc and GalNAc show cross peaks to three ring protons, H1, H2, and H3, while the α anomer, and indeed most of the analogs examined, show only two cross peaks to H2 and H3. Although N-sulfonation results in a significant change in

the ^{15}N chemical shift of GlcN, 6-O sulfo substitution has no apparent effect on the local environment of the amino nitrogen.

5. Conclusions

The work demonstrates the detection of ^{15}N in amino sugars through long-range couplings to carbon-bound protons of the sugar ring. Comparison of the ge-HMBC, IMPACT-HMBC and a modified IMPACT-HNMBC pulse sequence revealed improved sensitivity, resolution and reduced F_1 noise with the IMPACT-HNMBC experiment modified to remove ^1J-filters. Although this approach is less sensitive than using the HSQC experiment to measure ^{15}N chemical shifts through directly-bonded protons, the IMPACT-HNMBC experiment has the advantage of being applicable to molecules for which fast exchange precludes efficient detection of N–H resonances, for example in amino sugars containing an N-sulfo substitution or an unmodified amino group, common motifs in heparin and HS.

The compounds examined in this study are inexpensive and commercially available. Application of this approach to more complex oligosaccharides will likely require that the experiments be carried out on sub-milligram quantities of isolated material. Clearly the use of ^{15}N-specific labeling will be required to make such measurements practical. Additional instrumental improvements in S/N can also help increase the sensitivity of these measurements. The experiments reported herein used a 5-mm room temperature broad-band inverse probe. Additional gains in sensitivity could be achieved by performing the measurements in a higher magnetic field, using a cryogenically cooled probe or a microcoil probe with a reduced detection volume.

Appendix A. Supplementary material

Supplementary data associated with this article can be found, in the online version, at doi:10.1016/j.jmr.2011.01.029.

References

[1] D.L. Rabenstein, Heparin and heparan sulfate: structure and function, Nat. Prod. Rep. 19 (2002) 312–331.
[2] R.L. Jackson, S.J. Busch, A.D. Cardin, Glycosaminoglycans: molecular properties, protein interactions, and role in physiological processes, Physiol. Rev. 71 (1991) 481–539.
[3] I. Capila, R.J. Linhardt, Heparin–protein interactions, Angew. Chem., Int. Ed. 41 (2002) 390–412.
[4] G. Bodenhausen, D.J. Ruben, Natural abundance nitrogen-15 NMR by enhanced heteronuclear spectroscopy, Chem. Phys. Lett. 69 (1980) 185–189.
[5] A. Bax, R.H. Griffey, B.L. Hawkins, Correlation of proton and nitrogen-15 chemical shifts by multiple quantum NMR, J. Magn. Reson. 55 (1983) 301–315.
[6] G.E. Martin, R.C. Crouch, Inverse-detected two-dimensional NMR methods: applications in natural products chemistry, J. Nat. Prod. 54 (1991) 1–70.
[7] C. Sigulinsky, P. Babu, X.V. Victor, B. Kuberan, Preparation and characterization of ^{15}N-enriched, size-defined heparan sulfate precursor oligosaccharides, Carbohydr. Res. 345 (2010) 250–256.
[8] V. Tran, T. Nguyen, K. Raman, B. Kuberan, Applications of isotopes in advancing structural and functional heparanomics, Anal. Bioanal. Chem. 399 (2011) 559–570.
[9] C.D. Blundell, P.L. DeAngelis, A.J. Day, A. Almond, Use of ^{15}N-NMR to resolve molecular details in isotopically-enriched carbohydrates: sequence-specific observations in hyaluronan oligomers up to decasaccharides, Glycobiology 14 (2004) 999–1009.
[10] V.H. Pomin, J.S. Sharp, X. Li, L. Wang, J.H. Prestegard, Characterization of glycosaminoglycans by ^{15}N NMR spectroscopy and in vivo isotopic labeling, Anal. Chem. 82 (2010) 4078–4088.
[11] Z. Zhang, S.A. McCallum, J. Xie, L. Nieto, F. Corzana, J. Jiménez-Barbero, M. Chen, J. Liu, R.J. Linhardt, Solution structures of chemoenzymatically synthesized heparin and its precursors, J. Am. Chem. Soc. 130 (2008) 12998–13007.
[12] A. Bax, D. Marion, Improved resolution and sensitivity in ^{1}H-detected heteronuclear multiple-bond correlation spectroscopy, J. Magn. Reson. 78 (1988) 186–191.
[13] H. Fulcrand, C. Benabdeljalil, J. Rigaud, V. Cheynier, M. Moutounet, A new class of wine pigments generated by reaction between pyruvic acid and grape anthocyanins, Phytochemistry 47 (1998) 1401–1407.
[14] C.C. Shen, Y.S. Chang, L.K. Ho, Nuclear magnetic resonance studies of 5,7-dihyroxyflavonoids, Phytochemistry 34 (1993) 843–845.
[15] G.E. Martin, C.E. Hadden, Long-range ^{1}H–^{15}N heteronuclear shift correlation at natural abundance, J. Nat. Prod. 63 (2000) 543–585.
[16] D.S. Wishart, C.G. Bigam, J. Yao, F. Abildgaard, H.J. Dyson, E. Oldfield, J.L. Markley, B.D. Sykes, ^{1}H, ^{13}C and ^{15}N chemical shift referencing in biomolecular NMR, J. Biomol. NMR 6 (1995) 135–140.
[17] L. Kay, P. Keifer, T. Saarinen, Pure absorption gradient enhanced heteronuclear single quantum correlation spectroscopy with improved sensitivity, J. Am. Chem. Soc. 114 (1992) 10663–10665.
[18] A.G. Palmer, J. Cavanagh, P.E. Wright, M. Rance, Sensitivity improvement in proton-detected two-dimensional heteronuclear correlation NMR spectroscopy, J. Magn. Reson. 93 (1991) 151–170.
[19] T. Parella, F. Sanchezferrando, A. Virgili, Purge scheme for efficient suppression of direct responses in gradient-enhanced HMBC spectra, J. Magn. Reson. 112 (1995) 241–245.
[20] J. Ruiz-Cabello, G.W. Vuister, C.T.W. Moonen, P. van Gelderen, J.S. Cohen, P.C.M. van Zijl, Gradient-enhanced heteronuclear correlation spectroscopy. Theory and experimental aspects, J. Magn. Reson. 100 (1992) 282–302.
[21] J. Schleucher, M. Schwendinger, M. Sattler, P. Schmidt, O. Schedletzky, S.J. Glaser, O.W. Sørensen, C. Griesinger, A general enhancement scheme in heteronuclear multidimensional NMR employing pulsed field gradients, J. Biomol. NMR 4 (1994) 301–306.
[22] T.D.W. Claridge, I. Perez-Victoria, Enhanced ^{13}C resolution in semi-selective HMBC: a band-selective, constant-time HMBC for complex organic structure elucidation by NMR, Org. Biomol. Chem. 1 (2003) 3632–3634.
[23] J. Furrer, A robust, sensitive, and versatile HMBC experiment for rapid structure elucidation by NMR: IMPACT-HMBC, Chem. Commun. (Cambridge, UK) 46 (2010) 3396–3398.
[24] K.A. Farley, G.S. Walker, G.E. Martin, Long-range two-dimensional ^{1}H–^{15}N heteronuclear shift correlation at natural abundance using GHNMQC. A study of the reverse transcriptase inhibitor delavirdine, Magn. Reson. Chem. 35 (1997) 671–679.
[25] R.T. Williamson, N. Sitachitta, W.H. Gerwick, Biosynthesis of the marine cyanobacterial metabolite barbamide. 2: Elucidation of the origin of the thiazole ring by application of a new GHNMBC experiment, Tetrahedron Lett. 40 (1999) 5175–5178.
[26] K. Furihata, H. Seto, Constant time HMBC (CT-HMBC), a new HMBC technique useful for improving separation of cross peaks, Tetrahedron Lett. 39 (1998) 7337–7340.
[27] A.T. Phan, Long-range imino proton-^{13}C J-couplings and the through-bond correlation of imino and non-exchangeable protons in unlabeled DNA, J. Biomol. NMR 16 (2000) 175–178.
[28] D.-L.M. Tzou, A solid-state NMR application of the anomeric effect in carbohydrates: galactosamine, glucosamine, and N-acetyl-glucosamine, Solid State Nucl. Magn. Reson. 27 (2005) 209–214.
[29] S.L. Eldridge, L.A. Higgins, B.J. Dickey, C.K. Larive, Insights into the capillary electrophoresis separation of heparin disaccharides from nuclear magnetic resonance, pKa, and electrophoretic mobility measurements, Anal. Chem. 81 (2009) 7406–7415.
[30] P.E. Hansen, Isotope effects on chemical shifts of proteins and peptides, Magn. Reson. Chem. 38 (2000) 1–10.
[31] A. Lycka, P.E. Hansen, Deuterium isotope effects on ^{14}N and ^{15}N nuclear shielding in simple nitrogen-containing compounds, Magn. Reson. Chem. 23 (1985) 973–976.
[32] L. Yao, J. Ying, A. Bax, Improved accuracy of ^{15}N–^{1}H scalar and residual dipolar couplings from gradient-enhanced IPAP-HSQC experiments on protonated proteins, J. Biomol. NMR 43 (2009) 161–170.